Supporting Information

Kratzer et al. 10.1073/pnas.1320393111

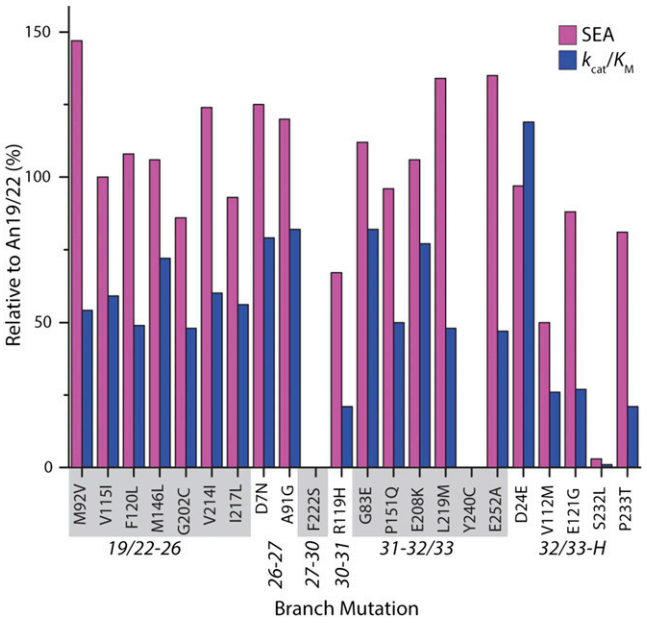

Fig. S1. Branch mutations that occur between An19/22 and the human uricase were individually inserted in An19/22 and assayed. Each of the 22 amino acid replacements (the number of replacements between An19/22 and the human uricase pseudogene) were assayed within the context of the An19/22 ancient protein to better understand the effects of individual mutations during mammalian uricase history. Each variant was characterized by the following properties: (*i*) the specific enzyme activity of the purified tetrameric variant (purple) and (*ii*) catalytic efficiency (i.e., k_{cat}/K_m) of the purified tetrameric variant (blue). All reported values are relative to the ancestral An19/22 enzyme. Two amino acid replacements, F222S and Y240C, prevented the purification of An19/22 variants and therefore their activity was not determined. The single S232L replacement could be purified, but its relative activity was severely diminished. Fig. 1 provides node numbers and branches.

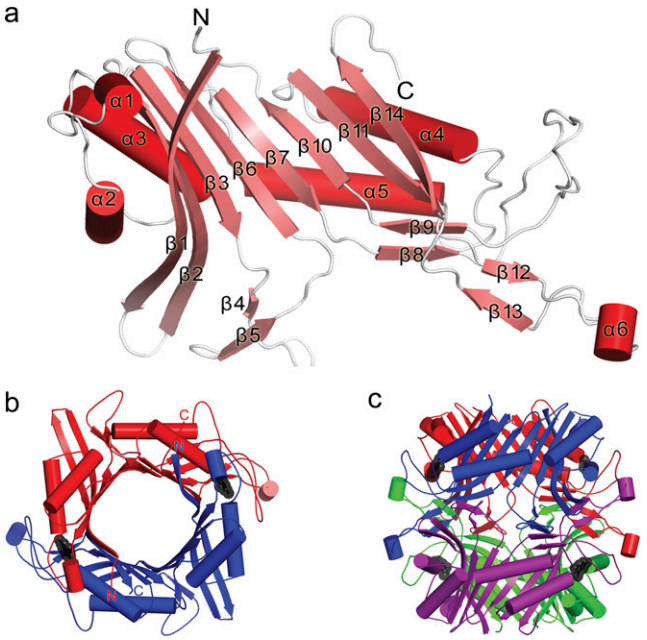

Fig. S2. Overall structure and tetrameric assembly of An19/22 uricase. Cartoon view of the uricase monomer (*A*), uricase dimer (*B*), and tetramer (dimer-of-dimers) (*C*). α-Helices and β-sheets are numbered based upon their position in the primary sequence, and the uricase monomers are colored red, blue, green, and purple. C, C terminus; N, terminus. Modeled ligand is shown as black sticks enclosed by transparent spheres. Image generated in PyMOL.

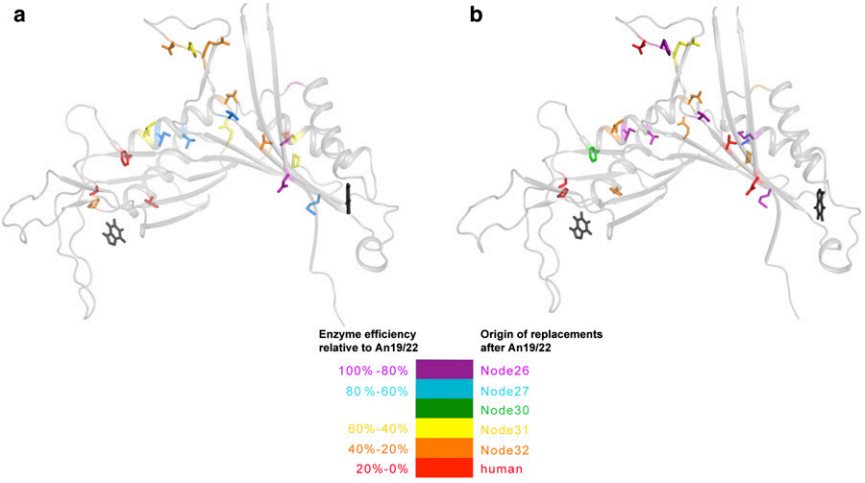

Fig. S3. The cluster effects of amino acid replacements on enzyme efficiency correlated with their evolutionary timings. The structure of An19/22 (shown as gray) oriented with the tetramer-buried side facing outward from the plane of view. The side chains of amino acid replacements that occur between A19/22 through human uricase are drawn as sticks and the substrate analog 8-azaxanthine ligand is shown in black sticks [modeled from Protein Data Bank (PDB) ID code 2YZD]. (*A*) Amino acid side chains colored by the percent reduction in catalytic efficiency relative to An19/22. Replacements having the least effect on catalytic efficiency are colored purple (those that retain 80% to 100% of relative efficiency), whereas replacements having the most detrimental effect on catalytic efficiency are colored red (i.e., those that retain only 20% or less of relative efficiency). (*B*) Side chains of amino acid replacements are colored by the node on the phylogenetic tree from which they occurred. The most ancient amino acid replacements occurred between An19/22 and An22 and are colored purple to compare with replacements having the least effect on catalytic efficiency from *A*. The most derived amino acid replacements occurred on the branch leading to humans and are colored red to match the color of the replacements from a that have the most detrimental effect on catalytic efficiency. The identity of colors at individual sites from *A* and *B* are correlated until node 30, where F222S occurred (the replacement that nearly abolishes enzyme activity).

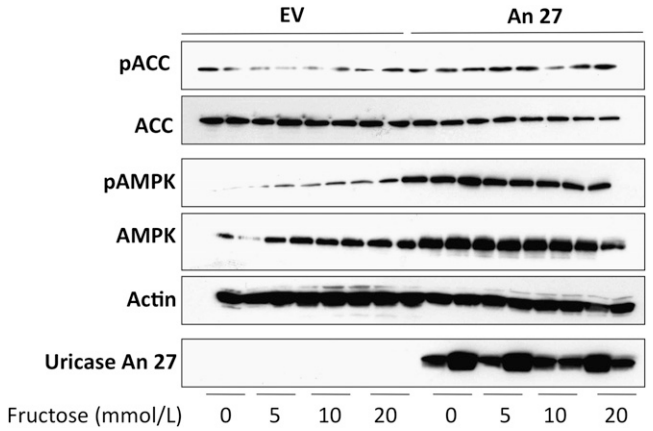

Fig. S4. Representative Western blot of lysates from HepG2 cells stably expressing an empty vector control or An27. ACC, Acetyl-Coa carboxylase; AMPK, AMP kinase; P, phosphorylated protein.

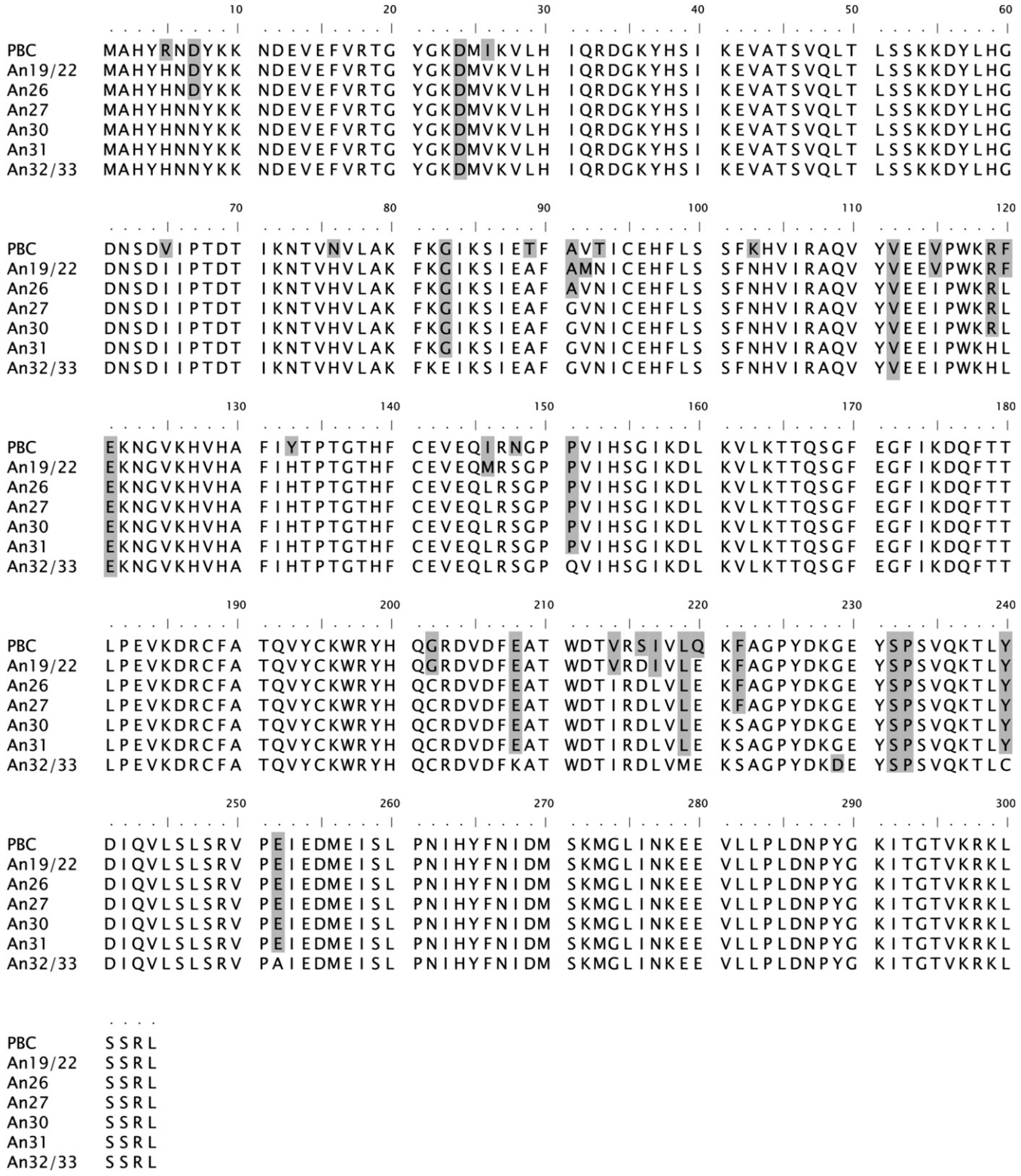

Fig. S5. Ancestral and chimera uricase amino acid sequences. The aligned sequences are labeled according to Fig. 1 in the article and shown in 10-residue blocks. Each sequence is 304 aa long. Also shown is the pig–baboon chimera (PBC) uricase that represents the protein component of the US Food and Drug Administration-approved pegloticase and is included in this alignment for reference. Residues that differ from the human pseudogene are highlighted in gray (except for the two premature stop codons at position 33 and 187).

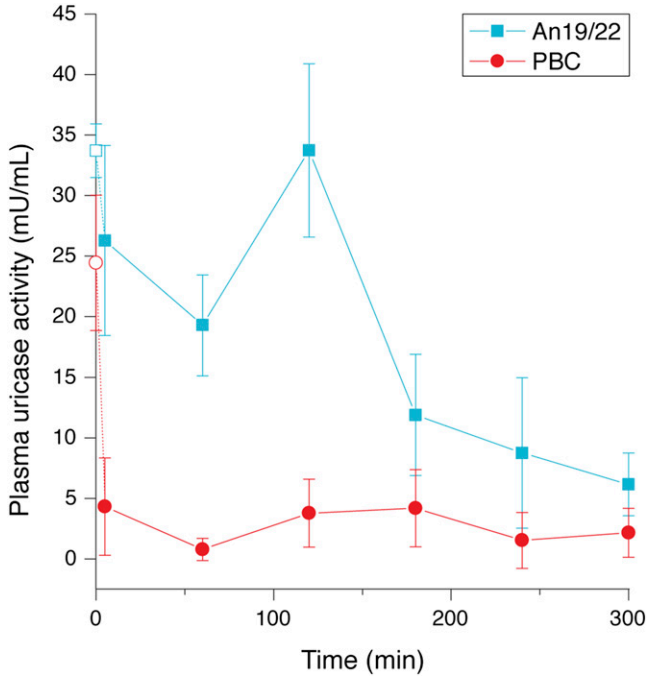

Fig. S6. Healthy rats injected with An19/22 displayed enhanced pharmacokinetics compared with the PBC uricase. Ten male Sprague–Dawley rats (five rats for each uricase) were each injected with 1 mL (0.2 mg/mL) of recombinant uricase preparations (An19/22 and PBC, the non-PEGylated form of pegloticase). One milliunit is the amount of uricase needed to oxidize 1 nM of urate per minute under assay conditions. The An19/22 uricase has a longer $t_{1/2}$ compared with PBC uricase. A Student *t* test was performed with a *P* value of 0.02.

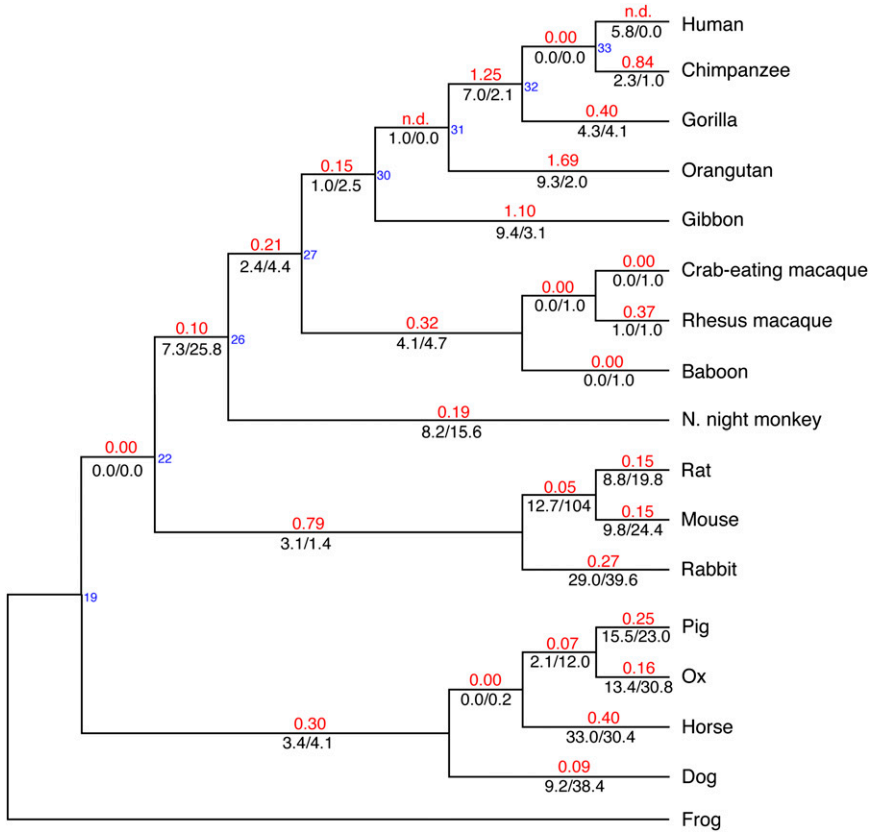

Fig. S7. Estimates of functional divergence across the uricase phylogeny. The cladogram shows estimates of nonsynonymous and synonymous substitutions, along with their associated ratios using a branch-based method. Nodes are labeled following Fig. 1 and colored blue. Nonsynonymous-to-synonymous ratios (dN/dS) are shown above their corresponding branches and colored red. Estimates of nonsynonymous and synonymous substitutions are shown, respectively, below each branch. Not determined (n.d.) represents cases in which the number of synonymous substitutions per synonymous site (denominator of dN/dS) is estimated to be zero.

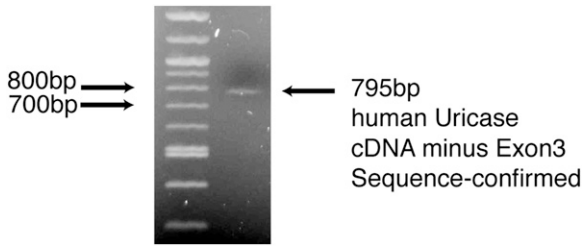

Fig. S8. cDNA of human uricase verified RNA transcription of the pseudogene in human fetal liver cells. Left lane shows ladder markers and right lane is the cDNA product of uricase transcripts. cDNA was gel-purified and sequenced to confirm uricase gene.

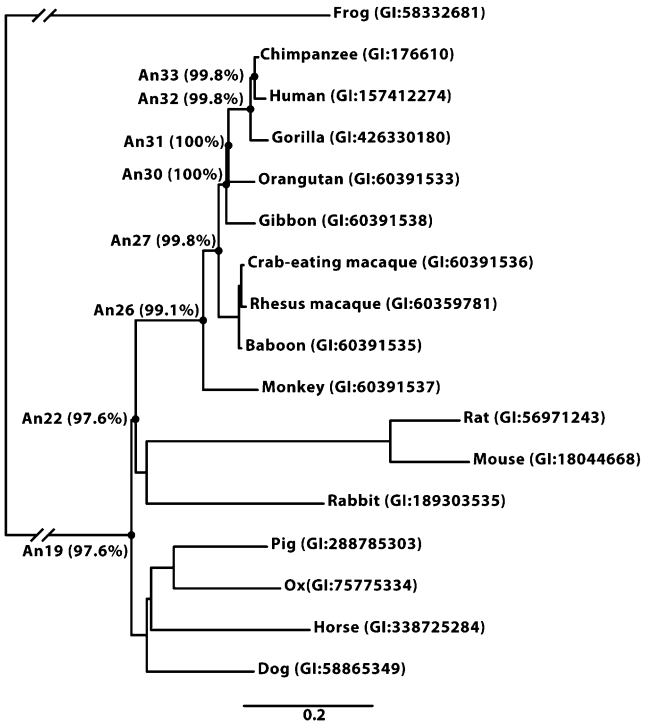

Fig. S9. Phylogram of uricases generated from a codon-based maximum likelihood analysis. The internal nodes are labeled with the posterior probability, a measure of statistical support, for each ancestral sequence inferred (note that these values are not nodal support). This phylogeny follows the inferred species tree for these organisms. The scale bar represents 0.2 replacements per site per unit evolutionary time. GenBank Identifier (GI) numbers are provided after each common species name.

Table S1. Data collection and refinement statistics

	UOX apo
Data collection	
Space group	$P6_1$
Cell dimensions	
a, *b*, *c*, Å	143.8, 143.8, 138.9
α, β, γ , °	90.0, 90.0, 120.0
Resolution, Å	39.8–2.40 (2.49–2.40)*
R_{sym} or R_{merge}	9.0 (47.6)
$I/\sigma I$	14.5 (3.2)
Completeness, %	100.0 (100.0)
Redundancy	5.2 (4.7)
Refinement	
Resolution, Å	2.40
No. reflections	63,465
R_{work}/R_{free}	20.7/25.9
No. atoms	
Protein	9,331
Ligand, ions	68
Water	196
β-factors	
Protein	53.3
Ligand/ions	59.5
Water	52.4
rmsds	
Bond lengths, Å	0.010
Bond angles, °	1.33

*Values in parentheses represent the highest resolution shell.